

Metal-ceramic interfaces: Overlayer-induced reconstruction and magnetism of 4d transition-metal monolayers

Ruqian Wu and A.J. Freeman

Department of Physics and Astronomy, Northwestern University, Evanston, Illinois 60208

(Received 3 October 1994)

Structural, electronic, and magnetic properties of metal-ceramic interfaces, $M/\text{MgO}(001)$ ($M=\text{Pd, Rh, and Ru}$), have been investigated using the full potential linearized augmented-plane-wave method. Ru and Rh monolayers are found to be able to retain large spin magnetic moments on $\text{MgO}(001)$ ($1.95\mu_B$ and $1.21\mu_B$ for Ru and Rh, respectively) — indicating, in principle, the potential application of $\text{MgO}(001)$ as a benign substrate for 4d monolayer magnetism. Significantly, according to our atomic-force determinations, the metal overlayers induce a sizable *buckling* reconstruction in the interfacial MgO layer, which enhances the $M\text{-MgO}$ binding energy by 0.1 eV. The weak $M\text{-O}$ interaction is mainly via tail effects; however, it affects the density of states at the Fermi level for $\text{Pd}/\text{MgO}(001)$ significantly and completely eliminates the small magnetic moment of the free Pd monolayer ($0.34\mu_B$).

Metal-ceramic interfaces are of great interest today because of their importance to both fundamental studies and practical applications.¹ Ceramics [especially $\text{MgO}(001)$] now appear to be promising benign substrates for the study of two-dimensional magnetism,³ especially since Li and Freeman² reported the giant magnetic moment of Fe on $\text{MgO}(001)$. [The Fe magnetic moment remains as large as $3.07\mu_B$ on $\text{MgO}(001)$, only $0.03\mu_B$ smaller than that for the free standing Fe monolayer.] In general, the weak interfacial interaction is considered to be via image charge and van der Waals mechanisms without significant chemical hybridization and charge transfer.⁴ As a result, the question naturally arises whether the predicted magnetism of 4d monolayers^{5,6} can also be sustained on the $\text{MgO}(001)$ substrate since it is known that 4d magnetism is very sensitive to small changes in the environment due to the larger spatial extent of its 4d wave function. Complex antiferromagnetic behavior with respect to the lattice expansion was reported for 4d transition metals by Moruzzi and Marcus.⁷ In free monolayer form, almost all 4d transition metals can be magnetic.⁶ Significantly, Ru and Rh monolayer magnetism is predicted to survive even on $\text{Ag}(001)$ or $\text{Au}(001)$ substrates,⁸⁻¹⁰ which appear to provide a way to realize 4d monolayer magnetism. However, since the surface energies of 4d transition metals are very close to those of Ag and Au, surface segregation may happen and thus result in the covering of the 4d film by a noble-metal monolayer. By taking this factor into account, we found that Ru magnetism survives in a $\text{Ag}/\text{Ru}/\text{Ag}(001)$ sandwich, while Rh and Pd are magnetically dead.¹⁰ This may well explain the lack of a magnetic signal in an experiment for $\text{Rh}/\text{Ag}(001)$.¹¹

In this paper, we explore the possible magnetism of Pd, Rh, and Ru monolayers on $\text{MgO}(001)$. Through full potential linearized augmented-plane-wave (FLAPW) total energy and atomic force calculations, we found indeed that Rh and Ru monolayers can sustain large magnetic

moments on $\text{MgO}(001)$, $1.21\mu_B$ and $1.95\mu_B$, respectively — indicating that $\text{MgO}(001)$ can be used, in principle, as a benign substrate to realize Ru and Rh magnetism. However, due to its sensitivity to the change of environment, magnetism of the Pd monolayer ($M=0.34\mu_B$) is quenched on $\text{MgO}(001)$ despite the weakness of the interfacial interaction.

The $\text{MgO}(001)$ substrate is simulated by a five layer slab, which has been proven to be sufficiently thick to reproduce the bulk MgO properties in the center layer.^{2,4} Assuming epitaxial growth, a pseudomorphic Pd, Ru, or Rh overlayer is put on top of the oxygen atoms on each side of the $\text{MgO}(001)$ slab to keep the symmetry (for computational convenience). In all calculations, we adopt the experimental lattice constant for bulk MgO for the lateral two-dimensional (2D) lattice constant, while the vertical positions of all the atoms are determined according to atomic forces.¹² In the FLAPW method,¹³ no shape approximations are made to the charge densities, potentials, and matrix elements. We employ the von Barth and Hedin formulas for the exchange-correlation potential.¹⁴ Energy cutoffs of 11 Ry and 70 Ry are employed for plane-wave bases and star functions to describe the wave function and charge density and potential in the interstitial region, respectively. Within the muffin-tin (MT) spheres ($r_{\text{MT,Rh\&Ru}} = 2.3$ a.u., $r_{\text{MT,O}} = 1.8$ a.u., $r_{\text{MT,Mg}} = 1.97$ a.u.), lattice harmonics with angular momentum l up to 8 are adopted. Summation over 15 k points in the $1/8$ irreducible 2D Brillouin zone is employed for k -space integrations. Test calculations with 28 and 36 k -points were also carried out for $\text{Ru}/\text{MgO}(001)$; no significant change was found in the total energy, atomic force, and magnetic moments. Self-consistency is assumed when the average root-mean-square distances between the input and output charge and spin densities are $2.5 \times 10^{-4} \text{ e}/(\text{a.u.})^3$ and $1 \times 10^{-4} \text{ e}/(\text{a.u.})^3$, respectively. This criterion assures the reliability of the total energy and force results up to 1 mRy.

DISCLAIMER

This report was prepared as an account of work sponsored by an agency of the United States Government. Neither the United States Government nor any agency thereof, nor any of their employees, make any warranty, express or implied, or assumes any legal liability or responsibility for the accuracy, completeness, or usefulness of any information, apparatus, product, or process disclosed, or represents that its use would not infringe privately owned rights. Reference herein to any specific commercial product, process, or service by trade name, trademark, manufacturer, or otherwise does not necessarily constitute or imply its endorsement, recommendation, or favoring by the United States Government or any agency thereof. The views and opinions of authors expressed herein do not necessarily state or reflect those of the United States Government or any agency thereof.

DISCLAIMER

**Portions of this document may be illegible
in electronic image products. Images are
produced from the best available original
document.**

and 2 mRy/a.u., respectively.

The vertical atomic positions determined through atomic force calculations are listed in Table I. As expected, the equilibrium distances between the interfacial oxygen and 4d overlayers are around 4.4–4.5 a.u. for all three transition metals. Significantly, both interfacial Mg and O atoms are pulled up from their positions in the ideal bulk MgO lattice ($d=7.95$ a.u.) and even show a sizable buckling ($\Delta d = 0.17$ a.u.). Since this structural change will affect other properties such as growth mode, bonding mechanism, magnetism, etc., experimental verification or refutation of this prediction is highly desired.

This buckling enhances the binding energy by about 0.1 eV/atom. As a result, the calculated binding energies for Pd, Rh, and Ru on MgO(001) are 0.69 eV, 0.84 eV, and 0.88 eV per adatom, respectively. They are significantly smaller than that on Ag(001) (i.e., ~ 2.8 eV per adatom) — indicating the weakness of the interfacial interaction between metal and ceramic. As expected, we found that large 4d magnetic moments can be sustained on MgO(001). As listed in Table I, the calculated spin magnetic moments for Rh ($1.21\mu_B$) and Ru ($1.95\mu_B$) are only 10% smaller than the corresponding values for their free standing monolayers ($1.45\mu_B$ and $2.14\mu_B$, respectively).

The weak free monolayer magnetism of Pd is entirely diminished, however, even on MgO(001) — demonstrating the sensitivity of Pd magnetism to the change of environment. This can be better understood from a comparison of the density of states (DOS) for the nonmagnetic Pd free monolayer (dashed line) and Pd/MgO(001) (solid line) plotted in Fig. 1. For the free Pd monolayer, the 4d band is very narrow due to the low coordination number, and the value of the DOS at E_F is about 5 states/eV per atom. Using the exchange integral result given by Janak¹⁵ ($J=0.34$ eV), the Stoner factor for the free Pd monolayer is 1.7 and thus results in a magnetic instability. However, the weak Pd-O interaction (mainly via the tail effects) reduces the DOS at E_F substantially to only 2.0 states/eV per atom. As a result, the Stoner factor decreases to 0.68, which is far smaller than unity and thus the nonmagnetic state is stable for Pd/MgO(001). By contrast, since for Ru and Ru monolayers their Fermi level lies in the middle of the d bands, the DOS at E_F for nonmagnetic states is less sensitive to change of environment. As a result, large magnetic moments can still survive in Ru/MgO(001) and Rh/MgO(001).

The calculated charge density for Ru/MgO(001) is

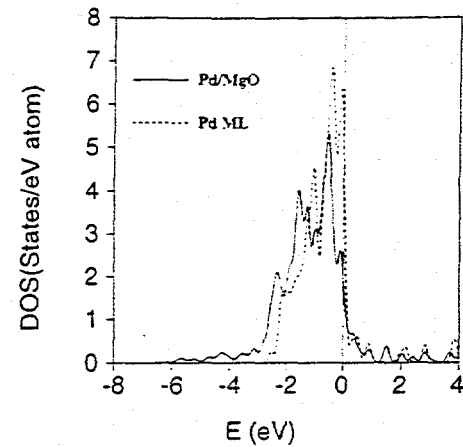


FIG. 1. The projected density of states of Pd monolayer in the free standing case (dashed line) and when adsorbed on MgO(001) (solid line).

plotted in Fig. 2(a). The strong ionic character of the O-Mg interaction is clearly shown whereas electrons are mainly around the O sites. Due to the screening effects, the bulklike character of the charge distribution is recovered even from the bottom half of the interfacial MgO layer. To understand better the Ru-MgO interaction, we give the charge density difference in Fig. 2(b) (i.e., $\Delta\rho = \rho_{\text{Ru/MgO}} - \rho_{\text{MgO}} - \rho_{\text{Ru}}$). Again, no significant change of charge distribution occurs in the interior region of MgO(001) (even from the subinterfacial MgO layer) due to screening effects. Since this behavior was also found in Rh/MgO(001) and in Ag/MgO(001) and Al/MgO(001) (Ref. 16) and Ag/CdO(001),¹⁷ it thus appears to signal a universal behavior at metal-ceramic interfaces.

Obviously, electrons are depleted from both Ru and O atoms and accumulate in the interstitial region (on top of Mg) in the Ru plane. This can be understood through Coulomb repulsion between tail electrons from Ru and O. When the Ru monolayer approaches MgO(001), charge density in the intermediate region between Ru and O(I) increases and so does their repulsive force. Since the attractive force from Ru and O nuclei is not strong enough (weak bonding) to balance this force, electrons are depleted away to the top of Mg where the charge density is smaller.

To answer the question whether interfacial oxida-

TABLE I. Calculated vertical positions (d , in a.u.), spin magnetic moments (M , in μ_B), and orbital magnetic moments ($\langle L_z \rangle$, in μ_B) for Pd, Rh, and Ru monolayers on MgO(001) and in the free standing case (values for M and $\langle L_z \rangle$ are given in parentheses).

Pd/MgO(001)				Rh/MgO(001)			Ru/MgO(001)		
Mg(I)	O(I)	Pd	Mg(I)	O(I)	Rh	Mg(I)	O(I)	Ru	
d	8.30	8.12	12.55	8.30	8.12	12.54	8.30	8.12	12.56
M	0.0	0.0	0.0 (0.34)	0.0	0.08	1.21 (1.45)	-0.01	0.07	1.95 (2.14)
$\langle L_z \rangle$	0.0	0.0	0.0 (0.1)	0.0	0.0	0.15 (0.26)	0.0	0.0	0.16 (0.15)

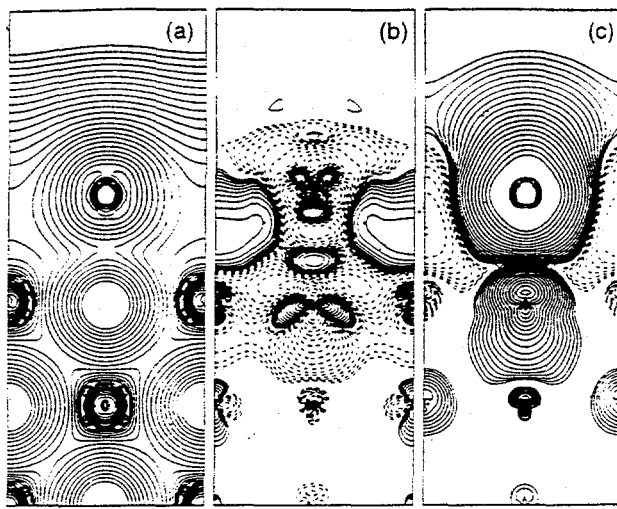


FIG. 2. The calculated (a) charge density, $\rho_{\text{Ru/MgO}}$, (b) charge density difference, $\Delta\rho = \rho_{\text{Ru/MgO}} - \rho_{\text{MgO}} - \rho_{\text{Ru}}$, and (c) spin density, $m_{\text{Ru/MgO}}$. Contours shown on the vertical (010) plane in (a) start from 1×10^{-4} e/a.u.³ and increase successively by a factor of $\sqrt{2}$, while in panels (b) and (c) they start from $\pm 1 \times 10^{-4}$ e/a.u.³ and increase successively by a factor of $\sqrt{2}$.

tion is involved at the Ru-MgO(001), we plotted in Fig. 3 the DOS projected into each muffin-tin sphere for Ru/Mg(001). Unlike those for the O(*I*-1) and O(*C*) layers, which exhibit large gaps around E_F , the DOS curves for O(*I*) extend far into the region above the top of the main 2p peaks even above E_F . In the panel for Ru, O-2p contributions can also be found under the bottom of the Ru-4d bands. However, these tail states are obviously small in magnitude. Thus we can say that the Ru-O interfacial interaction comes mainly via tail effects. Significantly, due to the charge depletion around O(*I*) [cf. Fig. 2(a)], the average potential around O(*I*) is lowered. Subsequently, the shoulder of the O(*I*)-2p band is pushed down by 0.9 eV compared to those for the interior O atoms. This may provide a way for experimentalists to check our theoretical predictions. Note also that the Mg states lie far above E_F and so do not affect the Ru-O interaction here.

In Fig. 3, the magnetic Ru (or Rh) overlayer induces a sizable exchange splitting at the O(*I*) site (0.2–0.3 eV). Even the DOS curves for the O(*I*-1) and O(*C*) layers are affected somewhat — indicating the long-range behavior of the magnetic perturbation as revealed for many systems.⁵ In Fig. 2(c), the spin density of Ru/MgO(001) shows considerable positive magnetization around O(*I*).

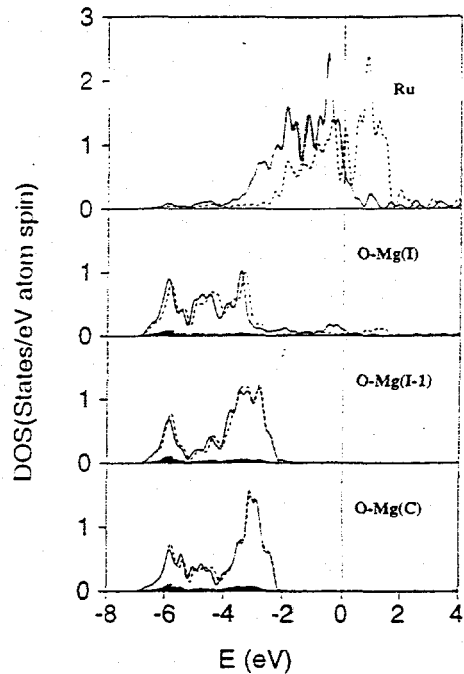


FIG. 3. The projected density of states of Ru and MgO layer (shaded regions for Mg) in Ru/MgO(001). Solid and dashed curves represent majority and minority spin parts, respectively.

Quantitatively, as listed in Table I, the induced magnetic moment for O(*I*) is about 0.07 – $0.08\mu_B$. On the other hand, although the area of positive spin density around Ru is somewhat squeezed by the MgO(001) substrate in Fig 2(c), the calculated spin magnetic moment of the Ru monolayer on MgO(001), as listed in Table I, is still as large as $1.95\mu_B$ — only 9% smaller than that for the free standing monolayer, $2.14\mu_B$. Similarly, a large magnetic moment ($1.21\mu_B$) is also sustained in Rh/MgO(001). If one adds their orbital magnetic moment (around $0.16\mu_B$), the net magnetic moments for Rh and Ru on MgO(001) are as large as about $1.4\mu_B$ and $2.1\mu_B$. Thus MgO(001) really also provides a benign substrate to realize two-dimensional Rh and Ru magnetism in the laboratory.

We thank S.D. Bader for his interest and for discussions. This work was supported by the Department of Energy under Contract No. DE-FG02-88-ER45372 and a computing grant from BES at the NERSC Lawrence Livermore National Laboratory.

¹See "Metal-Ceramic Interfaces," edited by M. Rühle, A.G. Evans, M.F. Ashby, and J.P. Hirth (Pergamon Press, New York, 1990).

²C. Li and A.J. Freeman, Phys. Rev. B **43**, 78 (1991).

³Y.Y. Huang, C. Liu, and G.P. Felcher, Phys. Rev. B **48**, 178 (1993).

⁴C. Li, R.-q. Wu, A.J. Freeman, and C.L. Fu, Phys. Rev. B **48**, 8317 (1993), and references therein.

⁵A.J. Freeman and R.-q. Wu, *J. Magn. Magn. Mater.* **100**, 497 (1992).

⁶S. Blügel, *Phys. Rev. Lett.* **68**, 851 (1992).

⁷V.L. Moruzzi and P.M. Marcus, *Phys. Rev. B* **42**, 10322 (1990).

⁸M.J. Zhu, D.M. Bylander, and L. Kleinman, *Phys. Rev. B* **43**, 4007 (1991).

⁹O. Eriksson, R.C. Albers, and A.M. Boring, *Phys. Rev. Lett.* **66**, 1350 (1991).

¹⁰R.-q. Wu and A.J. Freeman, *Phys. Rev. B* **45**, 7222 (1992).

¹¹G.A. Mulholland, R.L. Fink, and J.L. Erskine, *Phys. Rev. B* **44**, 2393 (1991); C. Liu and S.D. Bader, *ibid.* **44**, 12062 (1991).

¹²R.-q. Wu and A.J. Freeman (unpublished); R. Yu, D. Singh, and H. Krakauer, *Phys. Rev. B* **43**, 6411 (1991).

¹³E. Wimmer, H. Krakauer, M. Weinert, and A.J. Freeman, *Phys. Rev. B* **24**, 864 (1981); M. Weinert, E. Wimmer, and A. J. Freeman, *ibid.* **26**, 4571 (1982), and references therein.

¹⁴U. von Barth and L. Hedin, *J. Phys. C* **5**, 1629 (1972).

¹⁵J.F. Janak, *Phys. Rev. B* **16**, 255 (1977).

¹⁶T. Hong, J.R. Smith, and D.J. Srolovitz, *J. Adhesion Sci. Technol.* **8-9**, 1 (1994).

¹⁷F.Y. Rao, R.-q. Wu, and A.J. Freeman, *Phys. Rev. B* (to be published).